Calculations of local and gap modes in III-V semiconductors based on *ab initio* descriptions of the host crystals

David A. Robbie and Michael J. L. Sangster
J.J. Thomson Physical Laboratory, University of Reading, Reading RG6 6AF, Berkshire, United Kingdom

Pasquale Pavone
Institut für Theoretische Physik, Universität Regensburg, D-93040 Regensburg, Germany
(Received 28 December 1994)

Localized vibrations of substitutional impurities in III-V semiconductors are analyzed using three different models for the host crystals: the Keating model, the bond charge model, and a scheme based on recent *ab initio* calculations. The two empirical models lead to remarkably different predictions for local mode frequencies with results from the *ab initio* method lying in between. The host isotope fine structures of $^{12}C_{As}$ and $^{11}B_{As}$ local modes in GaAs are best accounted for in the calculations using the *ab initio* scheme. Estimates are made of the frequencies of some gap modes in AlAs and GaSb and of the width of fine-structure patterns in the latter.

I. INTRODUCTION

In a number of recent papers, simulations of local vibrational modes associated with light impurity atoms in III-V semiconductor host crystals have been used to model and interpret high-resolution measurements obtained by Fourier transform infrared spectroscopy: see, for example, Sangster *et al.*[1] and references to related work given in that paper. In these simulations the interatomic interactions in the host crystals have been represented by the Keating model[2] and local mode frequencies have been found as the highest eigenfrequencies for small clusters centered on the impurities and embedded in frozen crystal surroundings. After appropriate changes have been made for the atomic masses of the impurities, adjustments of the force constants around these defects have to be made to obtain agreement with experimental frequencies. Further information on force constant changes has been found by examining the fine structure of local mode lines arising from distributions of host atom isotopes: this approach was first used by Leigh and Newman.[3]

It was assumed in the earlier work[1] that the results obtained did not depend sensitively upon the model used for the host crystal as long as the high-frequency portion of the lattice mode spectrum was adequately represented. The main purpose of this paper is to demonstrate that this assumption is not true. This emerged in an attempt to extend the studies by using impurity gap modes as an additional source of information on force constant changes. Such extensions can clearly be carried out only for host crystals that display a gap between the acoustic and optical parts of the phonon spectrum. The model for the host must give a good fit to both limits of the gap as well as to the highest frequencies. The two-parameter Keating model is too simple to satisfy all these conditions and extensions to achieve these fits did not produce credible models. We then turned to the bond charge model (BCM) introduced by Weber[4] for homopolar semiconductors and extended for III-V applications by Rustagi and Weber.[5] For a simple model with few parameters this has been remarkably successful in reproducing experimental phonon dispersion curves including recent comprehensive neutron-scattering measurements for GaAs by Strauch and Dorner.[6] As we shall demonstrate in Sec. III, this model for GaAs produces results for local mode calculations that are dramatically different from those found with the Keating model. In particular, when the frequencies for $^{12}C_{As}$:GaAs local modes are calculated using the two models and allowing for changes of mass only (i.e., with no changes in force constants) the estimates differ by around 50 cm^{-1}. The adjustments to force constants, which then have to be made to secure agreement with experiment, are consequently very different in the two cases.

These conclusions raise important questions concerning the interpretation of force constant changes around impurities. A possible method for deciding between models for the host crystal would be to compare the deduced force constant changes with those obtained from *ab initio* defect calculations. (An illustration of this approach of linking empirical models to self-consistent calculations is the study of local modes from nitrogen defects in diamond by Sangster, Kiflawi, and Wood[7] which makes use of the *ab initio* work of Briddon, Heggie, and Jones.[8]) In the present paper another type of *ab initio* approach is adopted. Dispersion relations for semiconductors have been calculated by a density-functional linear-response technique by Giannozzi *et al.*[9] Their work included the III-V semiconductors GaAs, GaSb, and AlSb, for all of which neutron-scattering measurements are available, and AlAs, which cannot be grown as a bulk single crystal but which, in the form of an epitaxial layer, is of great interest as an end member of the range of AlGaAs mixed crystals. In the three cases for which comparisons with experiment are possible the agreement is extremely good. The method yields full dynamical matrices on a mesh of reciprocal-lattice vectors and, from

this, real-space interatomic force constants can be found by Fourier analysis. Thus a model for the perfect crystal can be deduced directly from the *ab initio* calculations, which, in effect, interpolates between the selection of reciprocal-lattice vectors for which the detailed calculations have been carried out. If the force constants describing the short-range interactions (i.e., without Coulombic contributions) decay sufficiently rapidly, the interpolation scheme is exact. Here the interpolation procedure is used as the best available model for the host crystals. Since the effective interatomic force constants are not restricted to a small number of neighbors and Coulombic terms are included, the cluster type of calculation that has been used for Keating models for host crystals is no longer convenient. Instead we use defect Green's-function techniques to deduce the localized mode frequencies. The perfect lattice Green's functions are found by standard methods from the frequencies and eigenvectors given by the *ab initio* interpolation scheme. Localized modifications to force constants are specified by changes in bond-stretch and bond-bending force constants: for easy comparison with earlier results, these changes within the defect space are described in terms of the Keating model.

The methods and procedures are discussed in the next section. We establish there that, when the Keating model is used, the implementation of the Green's-function techniques leads to results that are identical to those found earlier from cluster calculations. In Sec. III results are presented for the $^{12}C_{As}$ and $^{11}B_{As}$ local modes in GaAs, in Secs. IV and V local and gap modes in AlAs and GaSb are considered.

II. TECHNICAL MATTERS

In this section we first discuss briefly the three descriptions used for the host crystal. We then go on to the numerical techniques, which we use in later sections.

A. Models for the host crystal

1. Keating model

All our earlier work using cluster calculations[1,10] was based on the model introduced by Keating.[2] In its original version there were only two force constants: a stretch constant α and an angle bending constant β. The most obvious extensions to the model is to include an angle-angle correlation and, for III-V semiconductors, to allow for differences in the angle-bending constant at the two types of site. Coulomb forces can be added, but cannot be incorporated in the present version of our cluster program. The model and procedures for fitting to experimental data have been extensively discussed in our earlier papers and elsewhere.

2. Bond charge model

The BCM for GaAs that we have used in the calculations reported here is BCM5 in the paper by Strauch and Dorner.[6] (The parameters are listed in their Table 11 and the agreement with experiment for a closely related model is shown in their Fig. 6.) In the model covalent bonding is represented by an added charge on the nearest-neighbor bonds. For homopolar crystals this is placed at the midpoint,[4,11] but for III-V crystals the charge is placed closer to the group-V atom,[5] dividing the bond in the ratio 3:5.

3. Parametrization of ab initio calculations

Full details of the procedures for calculating phonon dispersion in semiconductors by the density-functional linear-response technique have been presented in the paper by Giannozzi *et al.*[9] The technique yields the full dynamical matrix at any selected wave vector **q** and can be adapted to give the dielectric tensor and the effective charges on atoms. These charges are used to extract the long-ranged Coulombic part of the dynamical matrix. From the remaining short-range parts calculated at a mesh of points in the symmetry reduced Brillouin zone, a set of (real-space) interatomic force constants is obtained by Fourier transformation. The set includes interactions between all pairs of atoms within a certain range. The interactions are included if, when one of the atoms is considered as the origin, the other is not outside an fcc Wigner-Seitz supercell (a rhombic dodecahedron) with linear dimensions four times larger than the corresponding primitive cell. When the second atom lies on a face, edge, or vertex at the surface of the supercell, an appropriate weighting factor is introduced to account for the number of shared surrounding supercells. The magnitudes of the force constants fall off with the interatomic separation but, to recover results at the restricted set of **q** points for which dynamical matrices have been calculated, it is important to include all of the terms within the supercell. This set of force constants together with the constants for the Coulombic interactions is then used as an interpolation scheme to provide eigenvectors and frequencies for all other **q** points. This is the procedure that was used in the original paper[9] to obtain phonon-dispersion relations. In this paper, in addition to the eigenfrequencies we require the eigenvectors from the interpolated matrices.

B. Numerical techniques

As mentioned in the Introduction, the cluster method, which was used earlier[1] for calculations of defect local mode frequencies based on Keating models for the host crystals, cannot readily be adapted for corresponding calculations based on either the BCM or *ab initio* descriptions of the host. We use instead standard Green's-function methods. In Sec. II B 1 we outline the steps in the calculation of the perfect lattice Green's functions that we will require.

One of our main interests will be in comparing the host isotope fine structures calculated on the basis of the three models. For the cluster simulations of the fine structure for C_{As} and B_{As} in GaAs reported earlier five calculations are required, one for each of the distinct arrangements of nearest-neighbor Ga isotopes (^{69}Ga and ^{71}Ga). The corresponding calculations using defect Green's-function methods again involve five separate runs with distinct

choices of mass changes in the nearest-neighbor contributions to the defect matrix. This is discussed in Sec. II B 2 and we show there that the earlier results for $^{12}C_{As}$:GaAs are recovered to high accuracy by this technique.

In Sec. II B C we discuss an approximate method for obtaining the fine-structure patterns as perturbations of a fully symmetric (T_d) arrangement of neighbors. This follows closely the work of Leigh and Newman.[3] We demonstrate, again for $^{12}C_{As}$:GaAs, that no significant loss of accuracy results from this treatment and, because of the great simplifications that it introduces, we use it in the analysis of fine structure patterns in Sec. III B.

1. Perfect lattice Green's functions

Green's functions for the pure host crystals have been defined and discussed in many standard works: see, for example, Maradudin *et al.*[12] and Bilz, Strauch, and Wehner.[13] Unfortunately, a variety of conventions for signs and phases is to be found. We adopt the following definition for the Cartesian Green's function relating the negative of the α component of the displacement response of an atom (lK), labeled by a cell index l and a species index K, to the β component of a sinusoidal force of frequency ω on an atom ($l'K'$):

$$G_{\alpha\beta}(lK;l'K';\omega)=\frac{1}{N(M_K M_{K'})^{1/2}} \times\sum_{\mathbf{q},j}\frac{w_\alpha(K|\mathbf{q}j)w^*_\beta(K'|\mathbf{q}j)}{\omega^2(\mathbf{q}j)-(\omega+i0)^2} \times\exp\{i\mathbf{q}\cdot[\mathbf{r}(lK)-\mathbf{r}(l'K')]\}\ , \quad (1)$$

where $w_\alpha(K|\mathbf{q}j)$ are normalized eigenvectors of the (Fourier-transformed) dynamical matrix for wave vector $\mathbf{q}$ and branch j [see Eq. (2.1.60) of Ref. 12]. Our definition of the Green's function agrees with that in Eq. 2.4.44b of Ref. 12 apart from an overall change of sign. The infinitesimal positive imaginary addition to ω yields the retarded Green's function when the sinusoidal time dependence is represented by $\exp(-i\omega t)$. The functions may be expressed in terms of their real and imaginary parts [cf. Eq. (8.4.14) of Ref. 12)]: the real part is the principal part of the above expression and the imaginary part is given by

$$\mathrm{Im}G_{\alpha\beta}(lK;l'K';\omega)=\frac{\pi}{N(M_K M_{K'})^{1/2}} \times\sum_{\mathbf{q},j}w_\alpha(K|\mathbf{q}j)w^*_\beta(K'|\mathbf{q}j) \times\exp\{i\mathbf{q}\cdot[\mathbf{r}(lK)-\mathbf{r}(l'K')]\} \times\delta(\omega^2-\omega^2(\mathbf{q}j)) \quad (2)$$

and is clearly zero outside the bands of allowed frequencies. The standard procedure for calculating these functions is to obtain first the imaginary part from a sample of wave vectors $\mathbf{q}$ in the reduced Brillouin zone and then to calculate the real part through the connection provided by the Kramers-Kronig relations. In our calculations we sample 3142 points in the symmetry-reduced ($\frac{1}{48}$) Brillouin zone and histogram the imaginary part into 800 bins equally spaced in frequency and covering the allowed bands. We shall denote the contribution to the ith bin, centered at $\omega_i=(i-\frac{1}{2})\Delta\omega$, where $\Delta\omega$ is the bin width, by $(\pi/2\omega)R^i_{\alpha\beta}(lK;l'K')$.

For our applications we are only interested in $G_{\alpha\beta}(lK;l'K';\omega)$ at frequencies *outside* the allowed perfect lattice phonon bands and, at these frequencies, the Green's functions are purely real and given by

$$G_{\alpha\beta}(lK;l'K';\omega)=\sum_{i=1}^{n}\frac{R^i_{\alpha\beta}(lK;l'K')}{\omega_i^2-\omega^2} \quad (3)$$

with the summation over the n bins. We shall need Green's functions for all atom pairs ($lK;l'K'$) for which the interactions will be modified by the presence of the defect. In all calculations reported here, this defect space is restricted to the site at which the impurity substitution takes place and its nearest neighbors. This defines a 15×15 Cartesian matrix Green's function, which we will write as $\mathbf{G}(\omega)$. In cases for which the defect has full T_d symmetry this can be exploited by choosing symmetry-adapted displacements and the corresponding Green's functions (which are particular linear combinations of the Cartesian functions). For determining the frequencies of localized modes in such cases only Green's functions of Γ_{15} symmetry are required.

2. Defect matrices for calculations of host isotope fine structure

Standard arguments show that $\mathbf{G}'(\omega)$, the defective lattice counterpart of the matrix Green's function $\mathbf{G}(\omega)$ introduced above, can be written as

$$\mathbf{G}'(\omega)=[\mathbf{I}+\mathbf{G}(\omega)\cdot\mathbf{D}(\omega)]^{-1}\mathbf{G}(\omega)\ , \quad (4)$$

where $\mathbf{D}(\omega)$ is the *defect matrix* that accounts for differences between the perfect and defective lattices. Here we have to consider differences in masses of atoms and also in force constants. For the latter, we express the differences in terms of changes in force constants of the Keating type: $\delta\alpha$, the change in the nearest-neighbor bond-stretching constant, and $\delta\beta$, the change in the (predominantly) bond angle constant with the impurity as apex. The extra forces introduced by the impurity act only on the impurity itself and its four nearest neighbors, i.e., only on atoms within the defect space. The construction of the 15×15 Cartesian defect matrix is discussed in the Appendix. The frequencies of localized modes, whether above the maximum lattice frequency or in a gap between acoustic and optic modes, are at poles in $\mathbf{G}'(\omega)$ and these are given by the condition

$$|\mathbf{I}+\mathbf{G}(\omega)\cdot\mathbf{D}(\omega)|=0\ . \quad (5)$$

Figure 1 shows this (15×15) determinant plotted as a function of frequency in the vicinity of the $^{12}C_{As}$:GaAs local modes with the Keating model for the host crystal and the force constant changes exactly as in the paper by Leigh *et al.*,[14] Figure 1(a) is for the C_{2v} arrangement of nearest-neighbor isotopes, two light and two heavy isotopes ($2l,2h$). The three crossings through zero at

582.4430, 582.6899, and 582.9362 cm^{-1} agree excellently with the corresponding results of Leigh *et al.*,[14] 582.4370, 582.6840, and 582.9303 cm^{-1}, respectively. Note that the splittings between the lines agree exactly to the quoted accuracy, but that there is an overall shift of 0.0059 cm^{-1}. This minor discrepancy can easily arise from the size of the bins ($\Delta\omega=0.375$ cm^{-1}) used in the histogram.

Figure 1(b) shows the corresponding plot for the $(3l,1h)$ case, one of the two arrangements with C_{3v} symmetry. The two higher frequencies of Fig. 1(a) now become degenerate. [The plot for the $(1l,3h)$ case is similar, with the degenerate modes at the lower frequency.] The two mode frequencies for the case illustrated are at 582.5864 and 582.9560 cm^{-1}, again in agreement with the cluster calculation apart from the small shift.

In Fig. 1(c) the full line shows the determinant for the triply degenerate $(4h)$ T_d symmetry case. Here the crossing through zero is a point of inflection at 582.4032 cm^{-1} (cf. 582.3973 cm^{-1} from the cluster calculations). For this T_d case we have also carried out the corresponding calculation using one of the three identical 3×3 Γ_{15} parts of the symmetry-adapted Green's-function matrix (see the Appendix). These results are also shown in Fig. 1(c) by the broken line, the frequency at which the determinant is zero agreeing exactly with the Cartesian result. Simplification would also have resulted from applying symmetry to the C_{3v} and C_{2v} cases, but we have not developed this. The T_d symmetry results are of particular importance in two ways: (a) for some host crystals that we shall be considering (e.g., AlAs) there is no choice of nearest-neighbor isotope and (b) in the approximate method for the host isotope fine structure, to be outlined in the following subsection, we expand about a fully symmetric arrangement of isotopes.

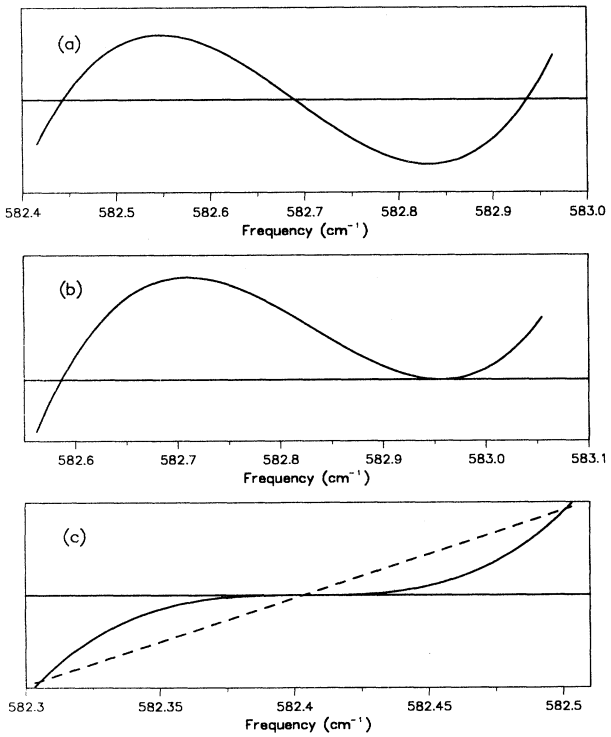

FIG. 1. Graphic solutions to Eq. (5): (a) for two light and two heavy $(2l,2h)$ Ga neighbors, (b) for $(3l,1h)$, and (c) for $(4h)$. Full lines are for Cartesian Green's functions and the broken line in (c) is for fully symmetrized Green's functions.

3. *Approximate method for the calculation of the isotope fine structure*

This method has been discussed by Leigh and Newman,[3] who point out the close similarities to earlier work on the theory of vibrations in molecules. They show that if for a particular arrangement of nearest-neighbor isotopes there is a local mode at frequency ω with eigenvector **u**, then, to first order, the change in frequency resulting from changes in the masses of the four neighbors is given by

$$\frac{\delta\omega}{\omega}=-\tfrac{1}{2}\sum_{n=1}^{4}\delta m_n\sum_{\alpha}u_{n\alpha}^2 \ . \tag{6}$$

The eigenvector components $u_{n\alpha}$ give the actual (i.e., not mass-reduced) displacements of the neighbors normalized in the conventional way:

$$\sum_n\sum_\alpha m_n u_{n\alpha}^2=1 \ , \tag{7}$$

where the first summation is now over *all* atoms in the crystal.

The particular unperturbed arrangement chosen has the full T_d symmetry with all four neighbors having the average mass of the two Ga isotopes, which we denote by m_{Ga}. All δm_n in Eq. (6) are then equal in magnitude. A choice has to be made from the degenerate eigenvectors. Leigh and Newman take the eigenvector with the impurity displacement in the z direction and write the displacement of the (111) Ga neighbor as $(v,v,w)/\sqrt{m_{\mathrm{Ga}}}$. Displacements of the other neighbors are related by symmetry. The expressions for the approximate fractional changes in ω for the various isotope arrangements are then given as follows: (i) T_d symmetry (all four masses changed by δm, which can be either positive or negative)

$$\frac{\delta\omega}{\omega}=-2(2v^2+w^2)\delta m/m_{\mathrm{Ga}} \ , \tag{8a}$$

(ii) C_{3v} symmetry (mass change δm on one neighbor, $-\delta m$ on the rest with δm again either positive or negative)

$$\frac{\delta\omega}{\omega}=\begin{cases}-(4v-w)w\delta m/m_{\mathrm{Ga}} & \text{(singlet)}\\ (3v^2+2vw+w^2)\delta m/m_{\mathrm{Ga}} & \text{(doublet)} \ ,\end{cases} \tag{8b}$$

and (iii) C_{2v} symmetry (mass change of δm on two neighbors and $-\delta m$ on the other two)

$$\frac{\delta\omega}{\omega}=\pm2(v+2v)v\delta m/m_{\mathrm{Ga}} \quad \text{or } 0 \ . \tag{8c}$$

In their treatment of the isotope fine-structure, Leigh and Newman[3] then found values for the eigenvector

terms v and w from a cluster calculation. As already stated, this route is also open to us for calculations based on the Keating model for the host crystal, but not for either the BCM or the models based on *ab initio* calculations. We therefore use an alternative method in which the contributions to the eigenvectors are given by the residues at the poles in the real parts of Green's functions at the local modes.

For a defective lattice the loss of translational symmetry means that the normal modes of vibration can no longer be classified by a wave vector $\mathbf{q}$ and a branch index j: we shall label them with a single index p. In Eq. (1) we make the following replacement for the α component of displacement of the atom (lK) in the pth mode:

$$(NM_K)^{-1/2}w_\alpha(K|\mathbf{q}j)\exp[i\mathbf{q}\cdot\mathbf{r}(lK)]\rightarrow\xi_\alpha(lK|p)$$

and the counterpart of Eq. (1) is then

$$G'_{\alpha\beta}(lK;l'K';\omega)=\sum_p\frac{\xi_\alpha(lK|p)\xi_\beta(l'K'|p)}{\omega_p^2-\omega^2}\ , \tag{9}$$

where the sum is over all $6N$ modes and we have noted that the eigenvector components are now all real. These elements of the defective lattice Green's-function matrix are, of course, found from the perfect lattice functions through Eq. (4). Near the frequency of a localized mode the term in the summation corresponding to the localized mode is dominant, the remaining contributions showing only a slow variation with frequency. By careful analysis close to the pole (which must be very precisely located) a value may be found for $\xi_\alpha(lK|p)\xi_\beta(l'K'|p)$ with p corresponding to the local mode. Individual eigenvector components, and hence the values of v and w, which we require, are then found by carrying out the process for different elements of the matrix $\mathbf{G}'(\omega)$ (using either the Cartesian form or the Γ_{15} part of the corresponding symmetry-adapted matrix).

As a check, we have compared the results for v and w found by this method with the terms in eigenvectors from cluster calculations (specifying the host lattice and defect modifications with identical Keating parameters). For $^{12}C_{As}$:GaAs and $^{11}B_{As}$:GaAs the values agree to better than one part in 25 000.

Finally, we compare the fine-structure pattern for $^{12}C_{As}$:GaAs calculated by this approximate method with the results from cluster calculations.[14] We find that the approximation gives results for the frequencies of the nine lines that are all marginally higher than the cluster results, the discrepancies all lying between 0.0012 and 0.0017 cm^{-1}. Note that this discrepancy is smaller than the 0.0059 cm^{-1} found in Sec. II B 2 to be the difference between the Green's function and the cluster calculations. Since the approximate method is also based on a Green's-function calculation for the unperturbed eigenvector, this improved agreement must be fortuitous. It arises mainly from choosing the unperturbed configuration to be that with all Ga nearest neighbors having the arithmetic mean mass. From Table 1 of Leigh *et al.*[14] it can be seen that, with this assumption, the central frequency is reduced by 0.0048 cm^{-1}, almost canceling the 0.0059 cm^{-1} attributed to binning error in the Green's-function method.

III. RESULTS FROM COMPARISONS OF THE THREE MODELS FOR GaAs

In Sec. III A we shall consider predictions of the local mode frequency for $^{12}C_{As}$:GaAs when only the change in mass of the impurity is taken into account. Then in Sec. III B we shall look for the additional changes in force constant required for reproduction of experimental results, including host isotope fine structure.

A. Calculations of $^{12}C_{As}$:GaAs local mode frequency using mass change only

When only the mass change of the C_{As} impurity is considered (and all four Ga nearest neighbors are taken to have the same mass) the defect space is restricted to the impurity itself and the matrices in the symmetry-adapted version of Eq. (4) are 1×1. The condition for a local mode Eq. (5) then becomes

$$1+[\mathrm{Re}G_{11}(\Gamma_{15}:\omega)](-\Delta m\omega^2)=0 \tag{10}$$

in the notation of the Appendix. The solution using the *ab initio* description of the host lattice is displayed graphically in Fig. 2: the intersection is at 527.14 cm^{-1}. The corresponding results for the Keating model and the BCM are very different: 498.33 and 551.27 cm^{-1}, respectively. It is clear from the forms of the intersecting curves in Fig. 2 that small changes in the high-frequency part of the Green's function can result in these major shifts in frequency. The most important difference between the models seems to be in the distinctions made between the Ga and As atoms. In our Keating model both are treated similarly apart from the minor difference in mass which leads to slightly preferential motion of the Ga atoms in high-frequency modes. This results in the perfect lattice self-Green's-functions for Ga and As atoms being very similar. On the other hand, in the BCM the added charge is placed closer to the group-V

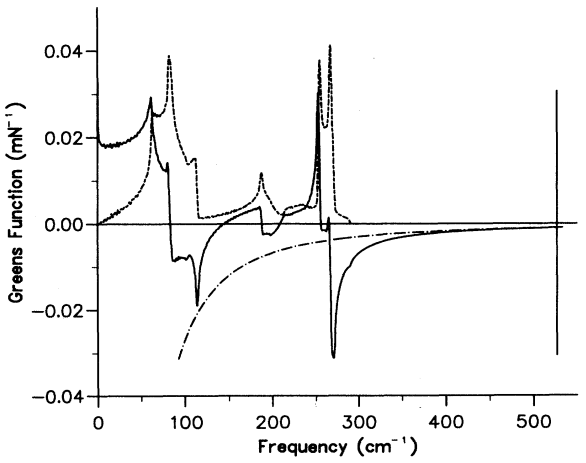

FIG. 2. Real (full line) and imaginary (dashed line) parts of $G_{11}(\Gamma_{15}:\omega)$, the perfect lattice Green's function for an As atom in GaAs from the *ab initio* calculations. The dash-dotted curve shows $(\Delta m\omega^2)^{-1}$ for a carbon impurity and the graphical solution of Eq. (10) is indicated by the vertical line.

atom (see Sec. II A 2) and this leads to a large enhancement of the motion of the As atoms in optic modes. This relates closely to the disagreement found by Strauch and Dorner[6] in GaAs between experimentally determined eigenvectors at the X point and those calculated from the BCM. As a consequence of this enhancement the high-frequency tail of the real part of the self-Green's-function for the As atom is accentuated and the frequency at which Eq. (10) holds is increased. Giannozzi *et al.*[9] show that their eigenvectors at the X point in GaAs agree with experiment. Since the local mode prediction from the same *ab initio* results falls between those from the other two models, it may be concluded that in GaAs there is some enhancement of the As motion in optic modes, but this is less extreme than that produced by the BCM.

Another less important difference between the models is that Coulombic interactions are ignored in the Keating model. This removes the splitting in the high-frequency peak of the imaginary part of the Green's function present in both BCM and *ab initio* calculations (see Fig. 2). The large differences that we have found for these three mass change calculations imply that the force constants required to obtain agreement with experiment will be very different in the three cases.

B. Fine structure on local modes in GaAs

As in earlier work[14] we consider changes in two force constants corresponding to bond stretching and bond-angle bending around the impurity. These changes are described in terms of the Keating model force constants α and β for ease of comparison with earlier work. The form of the defect matrix is given in the Appendix. We determine the two force constant changes $\delta\alpha$ and $\delta\beta$ for $^{12}C_{As}$ and $^{11}B_{As}$ in GaAs by fitting to (i) the measured frequency of the central line and (ii) the splittings between the components of the five line pattern. In our calculations using the approximate method of Sec. II B 3 the frequencies of all components of the pattern depend on only two parameters v and w in Eqs. (8). The implied relationships between the splittings are in accord with experiment (see Ref. 14).

In the first stage we make an arbitrary choice for $\delta\beta$ and find the change $\delta\alpha$ that gives the correct frequency for the central line. In these calculations we take all four Ga neighbors of the impurity to have the arithmetic mean mass since, in the approximate method, this gives the central frequency. Figure 3 shows combinations of $\delta\alpha$ and $\delta\beta$ that reproduce the central frequencies for $^{12}C_{As}$ (full line) and $^{11}B_{As}$ (broken line) when each of the three models for the GaAs host lattice is used. The expected differences between the models is readily apparent.

In Fig. 4 we present results, obtained by the approximate method discussed in Sec. II B 3, for the host isotope fine structure of the $^{12}C_{As}$ and $^{11}B_{As}$ local modes. In each part of the figure the horizontal lines give the experimentally measured frequencies. The broken lines show the calculated frequencies as functions of the force constant change $\delta\beta$, the change $\delta\alpha$ always being taken (as in Fig. 3) to give the correct value for the central component. The outer lines of the five line patterns are each found as weighted averages of three unresolved components as discussed in the paper by Leigh *et al.*[14] Figures 4(a) 4(b), and 4(c) give the results for $^{12}C_{As}$ based on the Keating, bond charge, and *ab initio* models, respectively.

As stressed in earlier calculations, the Keating model requires substantial stiffening of the bond-angle force constant to achieve the correct overall width of the fine-structure pattern (the constant β for the host crystal is 5.0775 $N\,m^{-1}$). In contrast, the BCM requires only a modest increase and when the Green's functions from *ab initio* calculations are used, an intermediate value (around 9.5 $N\,m^{-1}$) is needed. The fact that only a small change is needed for the BCM calculations is in line with the preferential strengthening of interactions around host As atoms. Again the *ab initio* results indicate that this strengthening is exaggerated in the BCM.

For Keating models it proved difficult to find force constant adjustments that gave simultaneous fits to all lines of the $^{12}C_{As}$:GaAs pattern (see Ref. 14). This is apparent in Fig. 4(a): the value of $\delta\beta$ required for a fit to the outer components is around 2.5 $N\,m^{-1}$ greater than that for the inner lines. There are similar difficulties with the BCM where the inner lines now require the larger change $\delta\beta$ [Fig. 4(b)]. All components are reproduced to high accuracy with a single change $\delta\beta$ when the *ab initio* Green's functions are used.

Figure 4(d) shows results for $^{11}B_{As}$ with all three models for the host crystal. The conclusions that may be drawn are similar to those for the ^{12}C impurity, but in all cases the values required for $\delta\beta$ are lower. An apparent difference between the two impurities is that whereas for

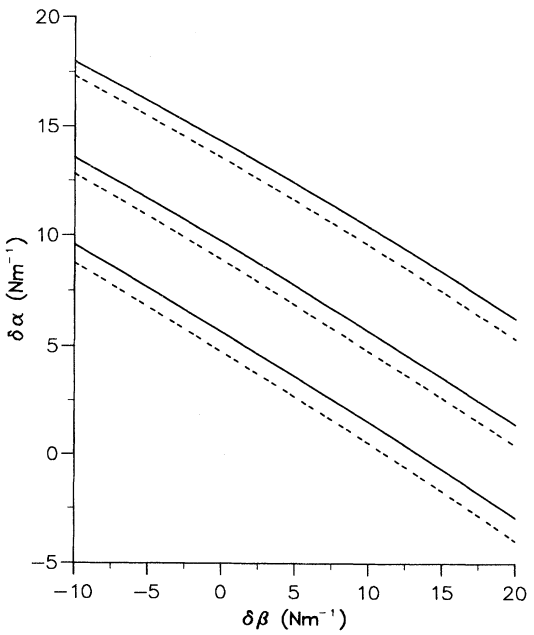

FIG. 3. Combinations of force constants $\delta\alpha$ and $\delta\beta$, which reproduce local mode frequencies for $^{12}C_{As}$ (full lines) and $^{11}B_{As}$ in GaAs (dashed lines). The upper, middle, and lower pairs of lines are for Keating, *ab initio*, and bond charge models, respectively.

^{12}C in all models both inner lines predict the same value for $\delta\beta$, this is not true for ^{11}B. (There is no such difference for the outer composite lines.) In fact the higher-frequency inner line for ^{11}B is poorly determined experimentally and an increase in the experimental frequency of under 0.01 cm^{-1} would remove this difference.

The negative change in $\delta\beta$ required for the BCM seems unrealistically large when compared with the corresponding Keating model β for the host crystal (5.0775 $N\,m^{-1}$). This may be due in part to the excessive strengthening of the interactions around the group-V atom in the BCM. Only a small negative change is required when the *ab initio* model is used.

In Ref. 14 it was found that, using values for $\delta\alpha$ and $\delta\beta$ obtained by fitting to the host isotope fine structure for the majority isotope, the impurity isotope shifts (^{13}C,^{12}C)

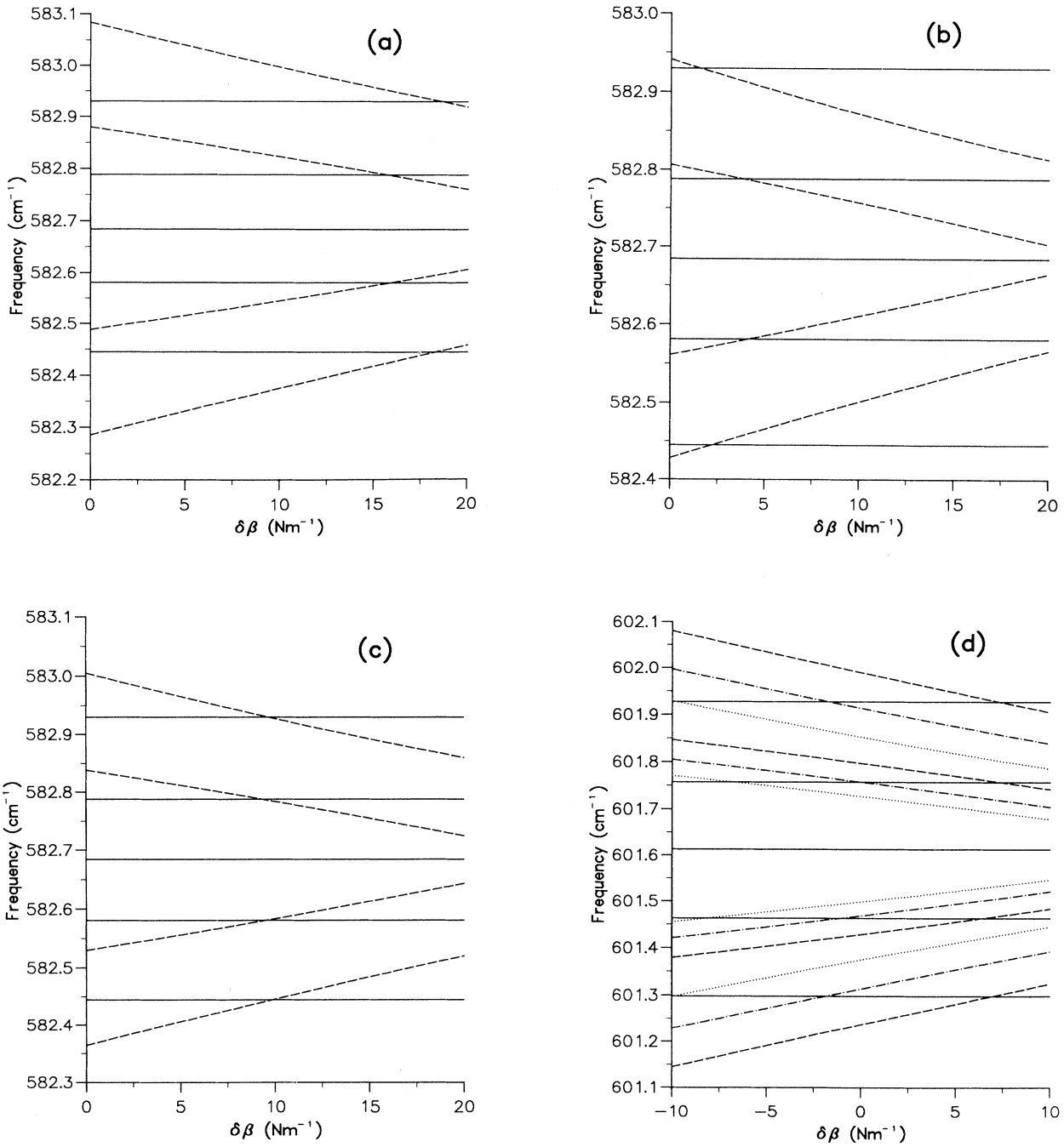

FIG. 4. Host isotope fine structure of local modes in GaAs: (a) $^{12}C_{As}$ with the Keating model for the host crystal: (b) $^{12}C_{As}$ (BCM); (c) $^{12}C_{As}$ (*ab initio*); (d) $^{11}B_{As}$ with Keating model (dashed line), BCM (dotted line), and *ab initio* model (dash-dotted line). Horizontal lines show the experimental values.

and (^{10}B,^{11}B) were too large by around 0.4 cm^{-1}. It was also shown that, if the interactions in the defective crystal can be described by a plausible harmonic model, these discrepancies should not have been found. This implies that a satisfactory explanation of both host and impurity isotope effects will require consideration of anharmonic effects. This conclusion would have been undermined if either the BCM or the *ab initio* models (both of them plausible harmonic models) had removed the discrepancies. In fact, the impurity isotope shifts produced by these models are all slightly larger than those reported in Ref. 14.

IV. LOCAL MODES AND GAP MODES FROM C IN AlAs

The characterization of defects in AlAs is of considerable recent interest due to the use of the material as a component in vertical surface emitting lasers.[15] AlAs is also of interest as an end member of the $Al_xGa_{1-x}As$ alloy sequence, which is of importance in heterostructure device fabrication. The material can only be grown by epitaxy, usually on a GaAs substrate, and has to be contained within sandwich layers. As a result, measurements of the phonon-dispersion relation by neutron scattering are not possible, although some information is available from Raman-scattering studies by Monemar.[16] AlAs was included in the range of semiconductors studied by Giannozzi *et al.*[9] and, in view of the success of their *ab initio* calculations for the closely related material GaAs, it is reasonable to assume that their procedure provides a good description.

For AlAs there is a gap in the density of modes between 216 and 332 cm^{-1} on the basis of the *ab initio* calculations. In principle, impurity modes localized with frequencies within the gap could act as a further source of information on force constant changes around defects. In this section we consider C_{As} in AlAs for which both local and gap modes occur. (We use the term local mode in the restricted sense of a mode with frequency above the maximum lattice frequency.) Since both constituents of AlAs have only one naturally occurring isotope, we are not concerned here with any of the host isotope fine-structure effects considered in Sec. III B: we shall return to these in Sec. V. No measurements of gap modes are available due to absorption by the substrate. The $^{12}C_{As}$:AlAs local mode has been detected by Davidson *et al.*[10] at 630 cm^{-1}.

The results of our calculations are displayed in the three parts of Fig. 5. Figure 5(a) is the AlAs counterpart of Fig. 3 and shows the combinations of the force constant changes $\delta\alpha$ and $\delta\beta$ that reproduce the measured local mode frequency for $^{12}C_{As}$:AlAs (630 cm^{-1}) when the host crystal is represented by the interpolation scheme deduced from the *ab initio* calculations.[9] The force constants are adjusted to ensure that condition (5) is satisfied at the measured frequency. The Green's-function matrix used is the 3×3 T_d symmetry-adapted matrix, as discussed in Sec. II B 2 and the purely real components of this matrix are found as before from Eq. (3). In Fig. 5(b), the frequency predicted for the gap mode for these sets of

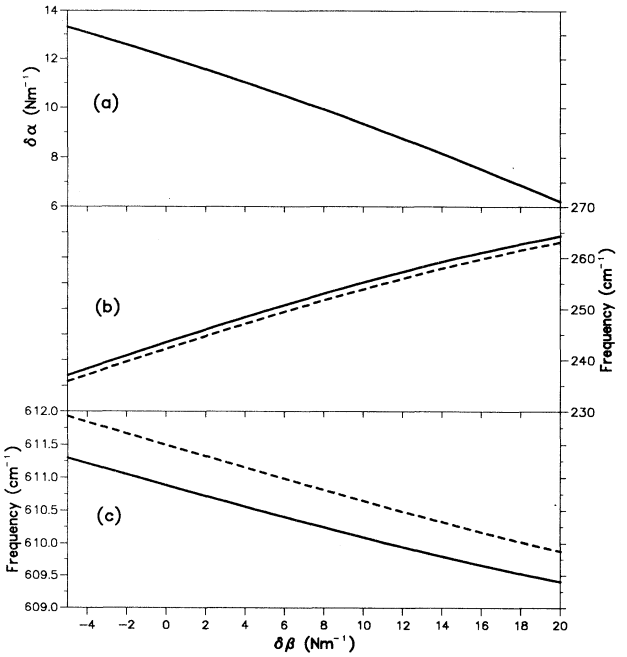

FIG. 5. Local modes and gap modes in AlAs: (a) combinations of force constant changes $\delta\alpha$ and $\delta\beta$, which reproduce the $^{12}C_{As}$ local mode frequency, (b) corresponding gap mode frequencies for $^{12}C_{As}$ (full line) and $^{13}C_{As}$ (dotted line), (c) $^{13}C_{As}$ local mode frequency from *ab initio* calculations (full line) and Keating model (broken line).

$\delta\alpha$ and $\delta\beta$ is shown as the full line. [The results are displayed as a function of $\delta\beta$, the corresponding values of $\delta\alpha$ being given in Fig. 5(a).] The prediction depends rather sensitively on the choice for $\delta\beta$, indicating that if measurements of both local and gap modes were available for a particular center they would accurately determine both stretch and angle force constant changes around the impurity. In the same part of the figure the predictions for the gap mode for the ^{13}C isotope is shown as a broken line. It is not surprising that the dependence on impurity isotope mass is so small: the light impurity participates very little in the mode. In Fig. 5(c), the frequency predicted for the $^{13}C_{As}$:AlAs local mode for the various choices of $\delta\beta$ [and the corresponding $\delta\alpha$ from Fig. 5(a)] is shown. As expected this is shifted substantially from the 630-cm^{-1} line for the ^{12}C isotope since the eigenvector in this case is dominated by the impurity displacement.

In an earlier paper[10] AlAs was modeled with a Keating model. We also carried out the above set of calculations with Green's functions obtained from this Keating model and found surprisingly little difference from the *ab initio* results. The counterparts of Figs. 5(a) and 5(b) would show practically no change from the figures presented and in the interests of clarity are not included. The predictions of the local mode frequency for ^{13}C:AlAs based on this Keating model are shown as the broken line in Fig. 5(c). The consistency between the two models is probably in large measure accidental since the limits of the gap in AlAs from the Keating model (205–321 cm^{-1}) are quite different from those found by the *ab initio* methods.

V. LOCAL MODES AND GAP MODES FROM IMPURITIES IN GaSb

Ab initio calculations of the phonon-dispersion relation for GaSb are also included in the paper by Giannozzi *et al.*[9] They found excellent agreement with the experimental data of Farr, Traylor, and Sinha.[17] For our purposes this crystal is of particular interest as both atoms are present in two isotopic forms: ^{69}Ga (60%) and ^{71}Ga (40%) as before and ^{121}Sb (57%) and ^{123}Sb (43%). Hence fine structure is to be found for substitutions on either site. No experimental information is available either on gap modes or on the fine structure of local modes in this material. Three examples of local modes are cited by Gaur, Vetelino, and Mitra[18] drawing on experimental work by Hayes,[19] Al_{Ga}:GaSb, P_{Sb}:GaSb, and As_{Sb}:GaSb, but the available spectroscopic techniques (and probably the quality of the crystal) did not allow for resolution of any fine structure. Of these three cases P_{Sb}:GaSb is the most likely candidate for having a gap mode. We find that when only the mass change is included, the predicted local mode frequency (321.2 cm^{-1}) lies very close to the measured frequency (324 cm^{-1}), but there is no gap mode. In order to obtain a gap mode with a simultaneous fit to the local mode frequency, the bond-angle force constant $\delta\beta$ has to be increased to at least 5 $N\,m^{-1}$ with a small compensating negative $\delta\alpha$. (The local mode frequency depends principally on $\delta\alpha$ and the gap mode frequency principally on $\delta\beta$.) This indicates that a gap mode is unlikely and, if it occurs at all, it will lie very close to the bottom of the gap.

In the absence of experimental results for comparison, we have carried out a few calculations to investigate what fine structure might be expected in gap modes. The gap in GaSb is narrow, lying between 161.4 and 182.9 cm^{-1} according to the calculations. We have considered a C_{Sb} impurity, treated first as a pure mass defect and then making force constant changes $\delta\alpha$ and $\delta\beta$ as for C_{As} in GaAs. We have used the full 15×15 Cartesian Green's-function matrix found from the parametrization of the GaSb *ab initio* calculations. As before, mode frequencies are found for the five distinct nearest-neighbor isotope arrangements and these give nine frequencies of which the highest three and lowest three are averaged into single lines, which we take to be unresolvable. For gap modes the decay of the eigenvector with distance from the impurity is much slower than that for the local mode and account should perhaps be taken of the different possible choices of second and further neighbors, but we have made no allowance for this. Results for the local and gap mode five line patterns are summarized in Table I.

TABLE I. Host isotope fine structure of local and gap modes in $^{12}C_{Sb}$:GaSb (frequencies in cm^{-1}).

			Mass change only		
local	483.95	484.09	484.21	484.33	484.47
gap	162.23	162.34	162.46	162.59	162.73
		Mass change, $\delta\alpha=5.85$ $N\,m^{-1}$, $\delta\beta=9.64$ $N\,m^{-1}$			
local	543.93	544.06	544.16	544.26	544.40
gap	165.68	165.87	166.07	166.27	166.49

The fine structure predicted for the local mode is similar to its counterpart in C_{As}:GaAs. The overall width is around 0.5 cm^{-1}, becoming slightly narrower when the force constant changes are introduced (principally due to the change $\delta\beta$) and the pattern is almost symmetric. For the gap mode the overall width is comparable, but becomes appreciably broader when the force constant changes are added. The result that the widths for gap and local modes are comparable is not an immediately obvious one. The displacement of the impurity is dominant in the local mode and small in the gap mode. From this one would expect the nearest-neighbor displacements to be of greater significance in the gap mode with a consequent increase in the width of the fine-structure pattern. However, this will be opposed by the reduction in the nearest-neighbor displacement implied by the slower decay with distance from the impurity of the gap mode eigenvector. The fine structure for the gap mode shows much less symmetry about the central line than that for the local mode: the lower-frequency components are more bunched together. This indicates that the approximate method used in some of our analysis of local mode fine structure would not be appropriate for gap modes. It should be noted that these gap modes lie close to the bottom of the gap (161.4 cm^{-1}). We have also investigated the substitution of a heavier atom on the Ga site In_{Ga}:GaSb, which gives a gap mode nearer the top of the gap (182.9 cm^{-1}). Allowing only for the mass change, we find a gap mode at 176.6 cm^{-1} with an overall width of about 0.3 cm^{-1}. The smaller width in this case is to be expected from the smaller *fractional* change in mass between the nearest-neighbor isotopes. The pattern is more symmetric than the C_{Sb} results given in the table, although there is some slight bunching, this time on the high-frequency side.

VI. CONCLUDING REMARKS AND SUMMARY

The main result to emerge from this work is that theoretical predictions of local mode frequencies depend to a surprisingly high degree on the model used for the host crystals. This sensitivity follows from the differences between the mode eigenvectors given by the various models. Even when empirical models predict lattice frequencies in excellent agreement with experiment, there is no guarantee that the corresponding eigenvectors, and hence the Green's functions, are correct. The same point was made very clearly in a paper by Leigh, Szigeti, and Tewary:[20] what is different in the present paper is the demonstration that models that have enjoyed widespread acceptance (such as the Keating model and the BCM) can produce such a wide range of predictions for defect mode properties. This is perhaps most clearly seen in Sec. III A where comparisons are made of predictions when only changes of mass are included. We are forced to conclude that, for the prediction of the properties of localized modes at least, empirical force constant models for the host crystal are not reliable. Only for methods based on *ab initio* calculations does agreement between calculated and measured dispersion relations provide a guarantee that eigenvectors, and therefore Green's functions, are

given to comparable accuracy. This is because the frequencies and eigenvectors are produced together from the full set of force constants that are the direct output of the *ab initio* calculations.

We have used standard Green's-function techniques (often described as the Lifshitz method) to incorporate existing and highly successful *ab initio* calculations for the dynamics of the perfect lattice into the analysis of vibrations in defective lattices. The elegance of the Lifshitz method lies in its exploitation of the translational symmetry of the perfect lattice to achieve major computational simplifications. Applications have generally been based on models such as the shell model or the BCM, but complete first-principles calculations of defect dynamics can also follow the same route. The first stage, finding the perfect lattice Green's functions, has been demonstrated here. The remaining step would involve evaluating force constant changes by consistent *ab initio* methods rather than adjusting to fit experimental data as we have done in this paper.

An approximate method for calculating the isotope fine structure is tested and used to demonstrate the superiority of the *ab initio* Green's functions in reproducing the fine-structure patterns for local modes.

The same methods are then used to investigate gap modes in AlAs and GaSb. These studies are necessarily speculative due to the absence of experimental data, but they indicate (a) how measurements of gap mode frequencies could serve to determine force constant changes and (b) the width of the fine-structure patterns of gap mode lines to be expected from host isotope effects.

ACKNOWLEDGMENTS

Paulo Giannozzi, Stefano de Gironcoli, and Stefano Baroni, the other authors of Ref. 9 on the *ab initio* calculations for III-V semiconductors, which form the basis of this paper, are thanked for their cooperation and in particular for allowing us to use the unpublished force constant parametrization of their results. We are also grateful to Roy Leigh, Ron Newman, and Dieter Strauch for their encouragement and helpful advice. D.A.R. thanks the former Science and Engineering Research Council (United Kingdom) for financial support during the tenure of which this work was carried out.

APPENDIX: GREEN'S FUNCTIONS AND FORCE CONSTANT MATRICES

Two types of Green's-function matrix (and the corresponding defect matrix) are considered in the main text: (a) Cartesian matrices and (b) symmetry-adapted matrices of which we generally require only the part transforming as the vector representation Γ_{15}. These matrices are required within the defect space of the substitutional impurity and its four neighbors. Details of the transformation matrices relating the 15×15 Cartesian matrices to their symmetrized counterparts are to be found in several places. Here we shall use the matrix transformation given by Bilz, Strauch, and Wehner[13] in their Table 22.3 corresponding to the symmetry-adapted displacements shown in their Fig. 22.4. The symmetrized Green's-function matrix has block diagonal form with the following blocks: (i) three equivalent 3×3 blocks corresponding to the three rows of the Γ_{15} representation

$$\begin{bmatrix} G_{11}(\Gamma_{15}:\omega) & G_{12}(\Gamma_{15}:\omega) & G_{13}(\Gamma_{15}:\omega) \\ G_{12}(\Gamma_{15}:\omega) & G_{22}(\Gamma_{15}:\omega) & G_{23}(\Gamma_{15}:\omega) \\ G_{13}(\Gamma_{15}:\omega) & G_{23}(\Gamma_{15}:\omega) & G_{33}(\Gamma_{15}:\omega) \end{bmatrix},$$

where the indices distinguish between the three occurrences of the representation in the labeling scheme of Ref. 13; (ii) a single diagonal Γ_1 element $G(\Gamma_1:\omega)$; (iii) two equivalent diagonal Γ_{12} elements $G(\Gamma_{12}:\omega)$; and (iv) three equivalent diagonal Γ_{25} elements $G(\Gamma_{25}:\omega)$.

When all four nearest-neighbor atoms are of the same isotope with mass difference δm_1 from the reference mass used in the Green's-function calculations, the full T_d symmetry is preserved. The corresponding blocks of the symmetrized defect matrix are then

(i)
$$\begin{bmatrix} 4\delta\alpha+2\delta\beta-\omega^2\delta m_0 & -2\delta\alpha-\delta\beta & \sqrt{2}(-2\delta\alpha+\delta\beta) \\ -2\delta\alpha-\delta\beta & \delta\alpha+\delta\beta/2-\omega^2\delta m_1 & \sqrt{2}\delta\alpha-\delta\beta/\sqrt{2} \\ \sqrt{2}(-2\delta\alpha+\delta\beta) & \sqrt{2}\delta\alpha-\delta\beta/\sqrt{2} & 2\delta\alpha+\delta\beta-\omega^2\delta m_1 \end{bmatrix},$$

(ii) $3\delta\alpha+\delta\beta/2-\omega^2\delta m_1$,

(iii) $2\delta\beta-\omega^2\delta m_1$,

(iv) $-\omega^2\delta m_1$.

The changes in nearest-neighbor force constants $\delta\alpha$ and $\delta\beta$ follow the usual Keating model description and δm_0 is the change in mass of the impurity atom.

The corresponding Cartesian matrices are readily generated by application of the transformation matrix listed by Bilz, Strauch, and Wehner.[13] This is still only for the fully symmetric isotope arrangement of nearest neighbors. For other choices of nearest-neighbor isotopes (which result in symmetry lowering) obvious adjustments to the mass changes in the diagonal terms have to be made, but no adjustments are made to the force constant changes.

[1]M. J. L. Sangster, R. C. Newman, G. A. Gledhill, and S. B. Upadhyay, Semicond. Sci. Technol. **7**, 1295 (1992).
[2]P. N. Keating, Phys. Rev. **145**, 637 (1966).
[3]R. S. Leigh and R. C. Newman, J. Phys. C **15**, L1045 (1982).
[4]W. Weber, Phys. Rev. Lett. **33**, 371 (1974).
[5]K. C. Rustagi and W. Weber, Solid State Commun. **18**, 673 (1976).
[6]D. Strauch and B. Dorner, J. Phys. Condens. Matter **2**, 1457 (1990).
[7]M. J. L. Sangster, I. Kiflawi, and G. S. Wood, Diamond Relat. Mater. **2**, 1243 (1993).
[8]P. R. Briddon, M. I. Heggie, and R. Jones, in *Proceedings of the Second International Conference on New Diamond Science and Technology, Washington, DC, 1990,* edited by R. Messier, J. T. Glass, J. E. Butler, and T. Roy (Materials Research Society, Pittsburgh, 1991), p. 63.
[9]P. Giannozzi, S. de Gironcoli, P. Pavone, and S. Baroni, Phys. Rev. B **43**, 7231 (1991).
[10]B. R. Davidson, R. C. Newman, D. A. Robbie, M. J. L. Sangster, J. Wagner, A. Fischer, and K. Ploog, Semicond. Sci. Technol. **8**, 611 (1993).
[11]W. Weber, Phys. Rev. B **15**, 4789 (1977).
[12]A. A. Maradudin, E. W. Montroll, G. H. Weiss, and I. P. Ipatova, in *Solid State Physics,* edited by H. Ehrenreich, F. Seitz, and D. Turnbull (Academic, New York, 1971), Suppl. 3, 2nd ed.
[13]H. Bilz, D. Strauch, and R. K. Wehner, in *Handbuch der Physik,* edited by S. Flügge (Springer, Berlin, 1984), Vol. 25/2d.
[14]R. S. Leigh, R. C. Newman, M. J. L. Sangster, B. R. Davidson, M. J. Ashwin, and D. A. Robbie, Semicond. Sci. Technol. **9**, 1054 (1994).
[15]M. Sugimoto, I. Oguru, H. Saito, A. Yasuda, K. Kurihara, H. Kosaka, and T. Numai, J. Cryst. Growth **127**, 1 (1993).
[16]B. Monemar, Phys. Rev. B **8**, 5711 (1973).
[17]M. K. Farr, J. G. Traylor, and S. K. Sinha, Phys. Rev. B **11**, 1587 (1975).
[18]S. P. Gaur, J. F. Vetelino, and S. S. Mitra, J. Phys. Chem. Solids **32**, 2737 (1971).
[19]W. Hayes, Phys. Rev. Lett. **13**, 275 (1964); Phys. Rev. **138**, 1227 (1965).
[20]R. S. Leigh, B. Szigeti, and V. K. Tewary, Proc. R. Soc. London A Ser. **320**, 505 (1971).